

Highlights

Discrete-Choice Model with Generalized Additive Utility Network

Tomoki Nishi, Yusuke Hara

- We propose utility functions for discrete-choice models using a novel neural-network architecture based on generalized additive models called GAUNet, and GAIUNet, which adds 2D interaction terms in addition to GAUNet.
- We develop MNL-GAUNet (multinomial logit model based on generalized additive utility network) and MNL-GAIUNet (multinomial logit model based on generalized additive and interactive utility network), which are MNL using GAUNet and GAIUNet, respectively.
- We compare our methods with ASU-DNN and MNL with linear utility functions using probe-person data collected in Tokyo, Japan. We show that our models achieve comparable accuracy to ASU-DNN and are more interpretable than previous models.

Discrete-Choice Model with Generalized Additive Utility Network

Tomoki Nishi^{a,*}, Yusuke Hara^{b,c}

^a*Toyota Central R&D Labs., Inc., 41-1, Yokomichi, Nagakute, 480-1192, Aichi, Japan*

^b*Tohoku University, 6-6-10 Aramaki Aza Aoba, Aoba-ku, Sendai, 980-8579, Miyagi, Japan*

^c*University of Tokyo, 7-3-1 Hongo, Bunkyo-ku, 113-0033, Tokyo, Japan*

ARTICLE INFO

Keywords:

Discrete-Choice Model
Multinomial Logit Model
Neural Network
Generalized Additive Model
Interpretability

ABSTRACT

Discrete-choice models are a powerful framework for analyzing decision-making behavior to provide valuable insights for policymakers and businesses. Multinomial logit models (MNLs) with linear utility functions have been used in practice because they are easy to use and interpretable. Recently, MNLs with neural networks (e.g., ASU-DNN) have been developed, and they have achieved higher prediction accuracy in behavior choice than classical MNLs. However, these models lack interpretability owing to complex structures. We developed utility functions with a novel neural-network architecture based on generalized additive models, named generalized additive utility network (GAUNet), for discrete-choice models. We evaluated the performance of the MNL with GAUNet using the trip survey data collected in Tokyo. Our models were comparable to ASU-DNN in accuracy and exhibited improved interpretability compared to previous models.

1. Introduction

Discrete-choice models (DCMs) are a powerful framework for analyzing and predicting decision-making behavior in various contexts to provide valuable insights for policymakers and businesses [26]. DCMs have supported policymakers and businesses for many years in practice while having been developed as theory-driven models based on the random utility theory after the random utility maximization model [18] was developed. These models are commonly used in marketing, transportation, urban planning, and other fields. DCMs can be used to analyze the effects of attributes on choice behavior, predict the choices, and evaluate the impact on different policy interventions or changes in the features of alternatives. The model is typically formulated with utility and choice probability functions. Analysts must decide the method of specifying the effect of each explanatory variable (e.g., linear utility function) and interaction between the variables before estimating the model.

In contrast to theory-driven DCMs, statistical machine-learning methods have been actively studied as data-driven methods in the information field [19]. Machine learning is roughly classified into two types: supervised and unsupervised. Supervised learning is a type of machine learning where an algorithm learns mapping between input data and output labels using a set of labeled training examples. Supervised learning aims to train a model to accurately predict the output labels for new unseen input data. On the other hand, unsupervised learning is a type of machine learning where an algorithm learns patterns in data without explicit supervision or labeled examples. Unsupervised learning aims to elucidate the structure or relationships in data that may not be apparent at first glance. The supervised-learning approach can be applied to predict decision-making behavior. The approach discovers the specification of the effect for each explanatory variable as a part of the process of training the model. Analysts cannot gain sufficient insight into physical or behavioral interpretation from the trained parameters, as the model is not derived from any decision-making theory.

With the rise of the fields of machine learning and AI, research on DCMs using machine learning has received considerable attention since 2017 [2]. Many of the early studies mainly aimed at proposing methods with higher prediction accuracy compared to multinomial logit (MNL) models; however, hybrid methods that aim to combine the best of both discrete-choice and machine-learning methods have been proposed. Wang et al. [28] proposed ASU-DNN, which learns the utility function for each alternative using a neural network (NN). The model achieved more accurate prediction than previous methods because of the nonlinear utility function with higher-order interactions between explanatory variables for each alternative. However, understanding the role of each variable is difficult owing

*Corresponding author

 nishi@mosk.tytlabs.co.jp (T. Nishi); hara@tohoku.ac.jp (Y. Hara)
ORCID(s): 0000-0001-8418-4633 (T. Nishi); 0000-0003-0268-9908 (Y. Hara)

to the complexity of the function. Sifringer et al. [25] proposed a linear MNL (L-MNL), which combines linear utility with MNL for the main factors and a NN to handle nonlinear utility for other additional factors. Han et al. [8] proposed TasteNet-MNL, which also learns the utility functions for the main factors for each alternative with the MNL-Linear and for individual attributes with NN. They reported that the model improves the accuracy of behavior prediction. The approach maintains interpretability for key factors by assuming linear utility functions and achieves higher accuracy using the NNs. Methods that combine high prediction accuracy and interpretability using only NNs are scarce.

In this study, we developed utility functions using a novel neural-network architecture based on generalized additive models called generalized additive utility network (GAUNet). GAUNet represents utility functions using the generalized additive models [9], whose shape functions use the NNs for each alternative, while ASU-DNN represents utility functions using the fully connected DNN for each alternative. Our approach maintains interpretability for the effect of each explanatory variable by learning the utility function for each variable as a different function and achieves high accuracy using the NNs as the utility function. We also develop a generalized additive and interactive utility network (GAIUNet), which adds the interaction terms between two explanatory variables represented by fully connected NNs to GAUNet.

We demonstrated the multinomial logit model using GAUNet (MNL-GAUNet) and GAIUNet (MNL-GAIUNet). We evaluated our model with data collected in Tokyo, Japan, from 2018 through 2021. The models learned decision-making in choosing transport modes (e.g., train, bus, and car). Our models achieved prediction accuracy comparable to that of ASU-DNN and better interpretability than previous models.

The contributions of this study are as follows:

- a) We propose utility functions for DCMs using a novel neural-network architecture based on generalized additive models GAUNet, and GAIUNet, which adds 2D interaction terms in addition to GAUNet.
- b) We developed MNL-GAUNet and MNL-GAIUNet, which constitutes MNL employing GAUNet and GAIUNet.
- c) We compare our models to ASU-DNN and MNL with linear utility functions on probe-person data collected in Tokyo, Japan. We show that our models achieve accuracies comparable to that of ASU-DNN and are more interpretable than previous models.

The remainder of the paper is organized as follows: Section 2 reviews related work such as classical DCMs, supervised-learning approaches, and recent DCMs with NNs. After introducing previous approaches that helped prepare our models in section 3, we propose MNL-GAUNet and MNL-GAIUNet in section 4. We present an overview of the experiment with the probe-person data and parameter settings in section 5. Section 6 shows the results of experiments for prediction accuracy and interpretability. Concluding remarks and future research directions are given in section 7.

2. Literature Review

DCMs have been actively studied for many years since McFadden proposed random utility maximization[18]. DCMs, grounded in statistical theory, assume that decision-makers make the choices sampled from probability distribution calculated by their utility, which is the degree of preference for each alternative. The approaches focus on specifying the mechanism to understand how decision-makers make choices rather than predicting the choices[26]. Many variations of DCMs have been developed: multinomial logit (MNL)[18], probit[13], mixed logit (MXL)[17], cross-nested logit (CNL)[27], and latent-class forms (LCM)[6]. The models differ in their assumptions of decision-making processes or probability distributions. After selecting a DCM (e.g., travel time), the analyst must prepare explanatory variables (e.g., MNL). The variables have to be handcrafted using variable transform (e.g., $\exp(x)$ and $\ln(x)$) where nonlinear characteristics are necessary. In conventional DCMs such as MNL, the utility is often estimated by the weighted linear combination of the hand-crafted explanatory variables.

Supervised-learning approaches can also be used to model decision-making behaviors. The approaches learn the relationship between input and output labels using training data to predict/infer output labels for unseen input data: artificial NNs, support vector machines, decision trees, and Bayesian networks[19]. Standard supervised-learning methods mainly focus on prediction accuracy rather than understanding the first principles. Moreover, we receive no information about the preference of each alternative but only the prediction of the choices or their probability when we use these methods as the behavior choice model. Explainable artificial intelligence (XAI) frameworks, which examine whether the model has learned intuitively reasonable input-output relations, have recently received attention[7] such as activation maximization (AM)[3], local interpretable model-agnostic explanations (LIME)[23] and Shapley additive

Table 1

Discrete-choice models (DCMs) and machine-learning (ML) methods. DCMs can compute utility for each explanatory variable or at least for each alternative. ML methods can predict choice probability or behaviors. In DCMs, utility functions have three types: Handcrafted (e.g., MNL-Linear), automatically designed by NNs (e.g., MNL-GAIUNet and ASU-DNN[28]), and the hybrid between them (e.g., L-MNL[25] and TasteNet-MNL[8]).

	Computable				Utility Function		
	Utility		Choice		Low	Model Representation	High
	Explanatory Variable	Alternative	Probability	Behavior	Handcrafted	Hybrid	Auto-Design by NN
Discrete Choice Model	✓	✓	✓	✓			
		✓	✓	✓			
Machine Learning			✓	✓			

◆ Handcrafted individual-specific variable □ NN Artificial Neural Network

◇ Handcrafted explanatory variable ○ Weighed sum operator

explanations (SHAP)[15]. XAI approaches focus on understanding the behavior of the trained model not the first principles of the input-output relationship.

MNL, whose utility functions are automatically designed by NN, have recently been developed: ASU-DNN[28], L-MNL[25], and TasteNet-MNL[8]. ASU-DNN separately estimates the utility of each alternative using a fully connected NN. The method achieved higher prediction accuracy than the conventional DCMs and ML methods. Meanwhile, the method must be applied post-processing, such as sensitivity analysis, to interpret the effect of each explanatory variable. L-MNL learns the utility of main factors using MNL-Linear and one of the other factors using a fully connected NN. The model learned using L-MNL provides the understanding of the main factors due to the MNL-Linear but makes us struggle to understand the other factors without post-processing because of the NN. TasteNet-MNL learns utility through the MNL-Linear using hand-crafted explanatory variables for the main factor and NN-learned ones for the decision-maker attributes. Our MNL-GAIUNet learns the utility for each explanatory variable in each alternative separately using NN. We can easily interpret the preference for each variable because the utility of each variable can be computed independently of other variables. MNL-GAIUNet also learns the utility for 2D interaction between the explanatory variables using NNs in addition to MNL-GAIUNet.

We summarize the comparison of MNL-GAIUNet with previous approaches mentioned above in Table 1. DCMs estimate the behavioral choices through utility, while ML methods directly predict the choices or their probability without the utility. The MNL-Linear estimates utility using the weighted linear combination of hand-crafted explanatory variables. On the other hand, brand-new MNLS using NN, such as ASU-DNN and L-MNL, learn all or part of the utility function using NNs. Therefore, the newer MNLS improve model representation more than the MNL-Linear. Our MNL-GAIUNet improves interpretability by learning the utility function for each variable using independent NNs.

We can also analyze MNL-GAIUNet in the context of generalized additive models (GAMs)[9]. GAMs are a flexible and powerful class of statistical models that extend the concept of generalized linear models (GLMs)[21]. While GLMs assume that the relationship between explanatory variables and the outcomes is linear, GAMs, modeled by the weighted

sum of nonlinear shape functions, allow for nonlinear relationships. Lou et al. proposed GA²M, which introduces an interaction term into GAM. GA²Ms using modern shape functions have been developed. Explainable boosting machine (EBM) [22] and GAMI-Net [29] are GA²M using gradient boosting trees and NNs as shape functions, respectively. Our MNL-GAIUNet (or MNL-GAIUNet) can be regarded as the MNL using GAM (or GA²M), whose shape functions are NNs, as the utility function for each alternative.

3. Preliminaries

This section introduces MNLs and GAMs.

3.1. Multinomial Logit Model

DCMs are statistical models that analyze decision-making behavior in situations where people choose an alternative from the set of available alternatives \mathcal{A} . DCMs assume that individuals make choices based on their preferences, called utility, for the alternatives themselves and their characteristics. Using statistical models, DCMs aim to represent the relationship between characteristics and individual choices. Random utility maximization (RUM) is the fundamental concept in DCMs, which assumes that individuals make choices by maximizing their utility.

Let $\mathcal{A} = \{1, \dots, K\}$ be set of the alternative index. DCMs treat two types of inputs: alternative-specific variables (e.g., travel time) $\mathbf{x}_{i \in \mathcal{A}} := [x_{i1}, \dots, x_{iN}]^\top$ and individual-specific variables (e.g., income) $\mathbf{z} := [z_1, \dots, z_M]^\top$, where N and M are the number of variables, respectively. In DCMs, the utility of each alternative U_k is formulated as the sum of the deterministic utility V_k and random utility ε_k as follows:

$$U_k(\mathbf{x}_k, \mathbf{z}) := V_k(\mathbf{x}_k, \mathbf{z}) + \varepsilon_k, \quad \forall k \in \mathcal{A}. \quad (1)$$

For simplicity, we omit the individual variable \mathbf{z} from our formulation. We can easily extend the following formulation to the one with the individual-specific variables.

According to RUM, individuals select the alternative with the maximum utility: $i^* = \arg \max_{i \in \mathcal{A}} U_i$. The probability that the individual selects alternative i is

$$\begin{aligned} P_i &= \text{Prob}(U_i > U_j), \quad i, \forall j \neq i \in \mathcal{A} \\ &= \text{Prob}(V_i + \varepsilon_i > V_j + \varepsilon_j) \\ &= \text{Prob}(V_j - V_i > \varepsilon_j - \varepsilon_i) \end{aligned} \quad (2)$$

The choice model, in which $\varepsilon_{i \in \mathcal{A}}$ follows the Gumbel distribution, is known as the MNL. The choice probability maximizing the utility can be represented as the following softmax function:

$$\varepsilon_i \sim \text{Gumbel}(\varepsilon_i; 0, \mu), \quad i \in \mathcal{A}, \quad (3)$$

$$:= \frac{1}{\mu} \exp\left(-\frac{\varepsilon_i}{\mu}\right) \exp\left[\exp\left(-\frac{\varepsilon_i}{\mu}\right)\right], \quad (4)$$

$$P(i|\mathbf{x}) = \frac{\exp(V_i(\mathbf{x}_i))}{\sum_{i \in \mathcal{A}} \exp(V_i(\mathbf{x}_i))}, \quad i \in \mathcal{A}, \quad (5)$$

where μ is a parameter of Gumbel distribution and \mathbf{x} is the set of the variables (i.e., $\mathbf{x} := \{\mathbf{x}_1, \dots, \mathbf{x}_K\}$). The proof is available in the book[26].

The deterministic utility function can be approximated using any function. For example, MNL with a linear utility function (MNL-Linear) applies a weighted sum of explanatory variables (hereafter used as a generic term for alternative- and individual-specific variables). The choice probability of MNL-Linear can be estimated as follows:

$$V_i(\mathbf{x}_i; \boldsymbol{\omega}_i) := \boldsymbol{\omega}_i^\top \mathbf{x}_i, \quad i \in \mathcal{A}, \quad (6)$$

$$P(i|\mathbf{x}; \boldsymbol{\omega}) = \frac{\exp(V_i(\mathbf{x}_i; \boldsymbol{\omega}_i))}{\sum_{i \in \mathcal{A}} \exp(V_i(\mathbf{x}_i; \boldsymbol{\omega}_i))}, \quad i \in \mathcal{A}, \quad (7)$$

$$\mathbf{x} := \{\mathbf{x}_i | i \in \mathcal{A}\}, \quad (8)$$

$$\boldsymbol{\omega} := \{\boldsymbol{\omega}_i | i \in \mathcal{A}\}, \quad (9)$$

where ω_i is the weight vector of the explanatory variables for the alternative i . Fukuda and Yai approximated utility using smoothing cubic spline[4]. ASU-DNN[28] adopts NNs as deterministic utilities. Both L-MNL[25] and TasteNet-MNL[8] use the linear function mainly and NNs as a supplement.

The weights can be estimated by maximizing the log-likelihood for data $\mathcal{D} := \{(y_1, \mathbf{x}_1), \dots, (y_D, \mathbf{x}_D)\}$, where (y_d, \mathbf{x}_d) is d -th data and $y_d \in \mathcal{A}$ is the chosen alternative index in d -th data:

$$\tilde{\omega} = \arg \max_{\omega} \sum_{(y_d, \mathbf{x}_d) \in \mathcal{D}} \ln P(y_d | \mathbf{x}_d; \omega), \quad (10)$$

where $\tilde{\omega}$ are the estimated weights. Various gradient methods can be used as the optimization methods: BFGS[12] in MNL-Linear and stochastic gradient descent approaches (e.g., Adam[10]) in MNL with NNs.

In conventional MNL analyses using MNL-Linear, weights for certain variables, such as travel time and distance, are frequently pooled across all alternatives to comprehend their universal characteristics. This shared weighting allows for estimating travel time utility that is agnostic to specific transportation modes. Conversely, weights that are unique to each mode facilitate the estimation of mode-specific utilities. The selection between these approaches is contingent upon the objectives of the analysis. When we apply some MNLS with neural-network approaches (e.g., ASU-DNN), we cannot analyze such universal characteristics because the utility for each variable cannot be calculated independently of the other variables owing to the network architectures.

3.2. Generalized Additive Models

Linear regression models (LRMs) have been widely used to model the linear relationship between an outcome y and the explanatory variables $\mathbf{x} = \{x_1, \dots, x_N\}$:

$$y = \beta_0 + \sum_j^N \beta_j x_j + \varepsilon, \quad (11)$$

where N is the number of the explanatory variables. β_0 and $\{\beta_1, \dots, \beta_N\}$ are the coefficients associated with the intercept and slope, respectively; ε represents the error term. The models implicitly assume that the error term is drawn from the normal distribution. LRMs cannot work well when assumptions of the linear relationship and the error term distribution are violated.

GLMs are the statistical models that relax the assumption of the error term distribution via a link function g :

$$\mathbb{E}(y) = g^{-1} \left(\beta_0 + \sum_j^N \beta_j x_j \right), \quad (12)$$

where $\mathbb{E}(y)$ denotes the expected value of y . By changing the link functions, GLMs can represent various regression models, such as Poisson and logistic regression. MNL-Linear can also be derived from GLMs by applying baseline category logit link functions $\ln(y_{i \in \mathcal{A}}/y_0)$, where y_0 is the outcome of the baseline category [1]. Estimating the parameters of GLMs involves maximizing the likelihood function represented by the probability of observing the training data.

GAMs are the statistical models that extend GLMs. While GLMs assume the relationships between the explanatory variables and the outcome projected by the link function, GAMs allow for nonlinear relationships as follows:

$$\mathbb{E}(y) = g^{-1} \left(\beta_0 + \sum_j^N \beta_j h_j(x_j) \right), \quad (13)$$

where $h_j(x_j)$ is a shape function for j -th explanatory variable. The smooth functions are typically represented using spline functions. Lou et al. developed the extended GAMs, called GA²M, which is the model that incorporates the interaction effects between two explanatory variables into GAMs [14]:

$$\mathbb{E}(y) = g^{-1} \left(\beta_0 + \sum_j^N \beta_j h_j(x_j) + \sum_{j,k \neq j}^N \beta_{jk} h_{jk}(x_j, x_k) \right). \quad (14)$$

The explainable boosting machine (EBM)[22], which is GA²M with gradient boosting tree as the shape functions, was developed. GAMI-Net uses NNs as shape functions [29]. EBM and GAMI-Net have been reported to have both high precision accuracy and explainability.

3.3. Artificial Neural Network

Artificial neural networks (ANNs) are supervised-learning frameworks that represent the relationship between the explanatory variables \mathbf{x} and the outcomes \mathbf{y} by repeatedly mapping using nonlinear functions[11]:

$$\mathbf{y}^{(l)} = h^{(l-1)} \left(\beta_0^{(l-1)} + \beta^{(l-1)\top} \mathbf{y}^{(l-1)} \right), \quad \forall l = 1, \dots, L \quad (15)$$

where L is the number of layers, $\mathbf{y}^{(0)} = \mathbf{x}$, $\mathbf{y}^{(L)} = \mathbf{y}$, and l is the layer index in the NN. Let $\beta^{(l-1)}$ and $\beta_0^{(l-1)}$ be the weight vector and intercept in $(l-1)$ -th layer, respectively. $h^{(l-1)}$ is the activation function. We often use some nonlinear functions as the activation functions: hyperbolic tangent $\text{Tanh}(\cdot)$, rectified linear function $\text{ReLU}(\cdot) = \max(0, \cdot)$ [20], and softmax function $\text{Softmax}(\cdot)$. MNL-Linear can be derived by using a single layer ($L = 1$) and the softmax function as the activation function h^0 , where \mathbf{y} is the choice probability vector of each alternative and \mathbf{x} is the explanatory variable. When we use categorical cross-entropy[24] as the loss function of the NN, the model is equivalent to MNL-Linear maximizing log-likelihood.

Recent MNLs with NNs have different neural-network architectures. Figure 1 shows the neural-network architectures of ASU-DNN, L-MNL, and TasteNet-MNL. In ASU-DNN, deterministic utilities of each alternative are learned using individual NNs. On the other hand, L-MNL learns the linear part of the utilities using the standard linear regression model and the nonlinear part using NNs. TasteNet-MNL uses NN to learn the nonlinear effects of the individual-specific variables and learns the deterministic utilities with the standard linear regression.

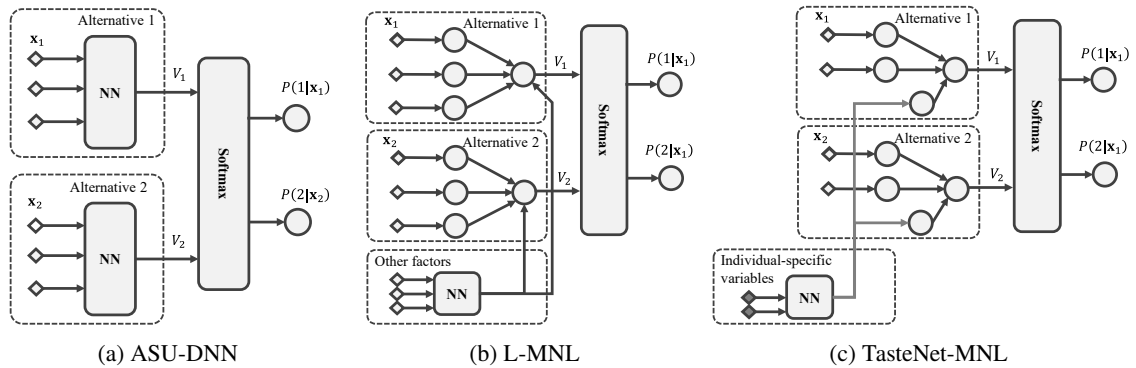


Figure 1: Multinomial Logit Model with Neural Networks. ASU-DNN learns deterministic utilities of each alternative using individual neural networks. On the other hand, L-MNL learns the linear part of the utilities using the standard linear regression model and the nonlinear part using the neural networks. TasteNet-MNL uses the neural network to learn the nonlinear effects of the individual-specific variables and learns the deterministic utilities with the standard linear regression.

We show the network architecture of GAMI-Net, which is the generalized additive model with NNs in Fig. 2(a). GAMI-Net uses NNs as the shape functions of GA^2Ms . It consists of a main effect module and a pairwise interaction module. The main effect module captures the effects of each alternative-specific variable and the pairwise interaction module captures the effects of the interaction between the two variables. Our MNL-GAIUNet is the MNL using GAMI-Net to estimate utilities for each alternative (Fig. 2(b)).

4. Discrete-Choice Model with Generalized Additive and Interactive Utility Network

4.1. Generalized Additive and Interactive Utility Network

We introduce two GAM-type utility functions using ANNs: GAUNet and GAIUNet. GAUNet is specified as the utility function by summing over each explanatory-specific utility represented by the NNs. GAUNet formulates the utility function for alternative $i \in \mathcal{A}$ as follows:

$$V_i(\mathbf{x}_i; \omega_i, \theta_i) := \text{ASC}_i + \sum_{j \in \mathcal{S}_i} \omega_{ij} \text{NN}_{ij}(x_{ij}; \theta_{ij}), \quad i \in \mathcal{A}, \quad (16)$$

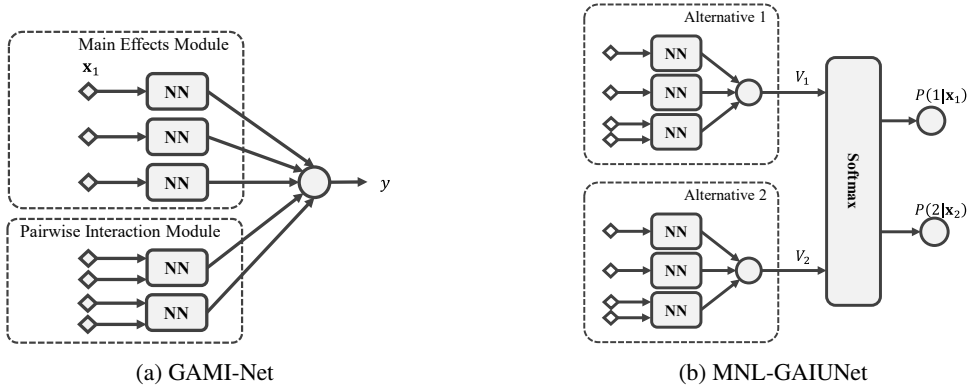

Figure 2: GAMI-Net and MNL-GAIUNet

Table 2

Comparison of GAUNet and GAIUNet with utility functions of previous studies. $SCS_i(\cdot)$ is the smoothing cubic spline, and \mathbf{z} is the vector explanatory variables other than $\mathbf{x}_i, \forall i \in \mathcal{A}$.

Methods	Formulation of Deterministic Utility Function
MNL-Linear	$ASC_i + \omega_i^\top \mathbf{x}_i$
Fukuda&Yai[4]	$ASC_i + SCS_i(\mathbf{x}_i)$
ASU-DNN[28]	$ASC_i + NN_i(\mathbf{x}_i)$
L-MNL[25], Taste-Net-MNL [8]	$ASC_i + \omega_i^\top \mathbf{x}_i + NN(\mathbf{z})$
GAUNet	$ASC_i + \sum_{j \in S_i} \omega_{ij} NN_{ij}(x_{ij})$
GAIUNet	$ASC_i + \sum_{j \in S_i} \omega_{ij} NN_{ij}(x_{ij}) + \sum_{(j,k) \in S_i^I} \omega_{ijk}^I NN_{ijk}(x_{ij}, x_{ik})$

where ASC_i is an alternative-specific constraint and ω_{ij} is the parameter of j -th explanatory variable for the alternative i . S_i is the set of explanatory variables for alternative i . $NN_{ij}(x_{ij}; \theta_{ij})$ is the NN that estimates the utility of j -th explanatory variable for the alternative i with network parameters θ_{ij} . In other words, the NN NN_{ij} depends only on the j -th explanatory variable. Let \mathbf{x}_i, ω_i , and θ_i be the vectors of the explanatory variables or parameters for the alternative i .

GAIUNet further considers the pairwise interaction term between explanatory variables in addition to GAUNet as follows:

$$V_i(\mathbf{x}_i; \omega_i, \omega_i^I, \theta_i, \theta_i^I) := ASC_i + \sum_{j \in S_i} \omega_{ij} NN_{ij}(x_{ij}; \theta_{ij}) + \sum_{(j,k) \in S_i^I} \omega_{ijk}^I NN_{ijk}(x_{ij}, x_{ik}; \theta_{ijk}^I), \quad i \in \mathcal{A}, \quad (17)$$

where ω_{ijk}^I and θ_{ijk}^I are parameters of the pairwise interaction terms between j -th and k -th variables for the alternative i . S_i^I is the set of considered pairs of explanatory variables. ω_i^I and θ_i^I are the vectors of parameters of the pairwise interaction terms for the alternative i . NN_{ijk} formulates the interaction among j -th and k -th explanatory variables.

We compare GAUNet and GAIUNet with four utility functions of previous studies in Table 2; MNL-Linear $ASC_i + \omega_i^\top \mathbf{x}_i$, Fukuda&Yai $ASC_i + SCS_i(\mathbf{x}_i)$, ASU-DNN $ASC_i + NN_i(\mathbf{x}_i)$, L-MNL/Taste-Net-MNL $ASC_i + \omega_i^\top \mathbf{x}_i + NN(\mathbf{z})$, where $SCS_i(\cdot)$ is the smoothing cubic spline, and \mathbf{z} is the vector explanatory variables other than $\mathbf{x}_i, \forall i \in \mathcal{A}$.

4.2. MNL-GAUNet

We introduce the MNL using GAUNet (MNL-GAUNet) as the deterministic utility function represented with Eq. (16). The choice probability for each alternative $i \in \mathcal{A}$ can be calculated as follows:

$$P(i|\mathbf{x}; \omega, \theta) = \frac{\exp(V_i(\mathbf{x}_i; \omega, \theta))}{\sum_{i \in \mathcal{A}} \exp(V_i(\mathbf{x}_i; \omega, \theta))}, \quad i \in \mathcal{A}. \quad (18)$$

We find the neural-network parameters ω and θ by maximizing the following objective function: $O(D; \omega, \theta)$ with respect to the data D :

$$\omega, \theta = \arg \max_{\omega, \theta} O(D; \omega, \theta), \quad (19)$$

$$O(D; \omega, \theta) := \text{LL}(D; \omega, \theta) + \alpha L_1(D; \omega), \quad (20)$$

$$\text{LL}(D; \omega, \theta) := \sum_{(y_d, \mathbf{x}_d) \in D} \log P(y_d | \mathbf{x}_d; \omega, \theta), \quad (21)$$

$$L_1(D; \omega) := \sum_{i \in \mathcal{A}} \sum_{j \in \mathcal{S}_i} |\omega_{ij}|, \quad (22)$$

where $L_1(\cdot)$ denotes L_1 norm for the weights of the NNs, and $\alpha(\leq 0)$ is the regularization parameter for the L_1 norm with a negative value. We can find the sparse solution for ω due to the L_1 norm. Stochastic gradient descent approaches such as Adam are often used to find the solution.

We define the importance score for each explanatory variable as follows:

$$\text{Imp}(x_{ij}; \omega, \theta) := \frac{\int_{\min(x_{ij})}^{\max(x_{ij})} \omega_{ij} v_{ij}(x_{ij}; \theta_{ij}) dx_{ij}}{(\max(x_{ij}) - \min(x_{ij}))}, \quad i \in \mathcal{A}, j \in \mathcal{S}_i, \quad (23)$$

We calculate $\text{Imp}(x_{ij}; \omega, \theta)$ using evenly partitioned values in the range of $\min(x_{ij})$ to $\max(x_{ij})$ because it would be difficult to calculate the integral directly. Our MNL-GAIUNet is equivalent to MNL-Linear when the number of the neural-network layers for all explanatory variables is one, and the activation functions are linear.

Unlike conventional methods such as ASU-DNN, our approach uses NNs to model the utility function of each variable independently, allowing us to analyze universal characteristics by pooling variable weights across all alternatives.

4.3. MNL-GAIUNet

We also develop the multinomial logit model with GAIUNet, in which the deterministic utility is specified in Eq. (17). The choice probability is derived as follows:

$$P(i | \mathbf{x}; \omega, \omega^I, \theta, \theta^I) = \frac{\exp(V_i(\mathbf{x}_i; \omega, \omega^I, \theta, \theta^I))}{\sum_{i \in \mathcal{A}} \exp(V_i(\mathbf{x}_i; \omega, \omega^I, \theta, \theta^I))}, \quad i \in \mathcal{A}. \quad (24)$$

We find the parameters by maximizing the following objective function $O(D; \omega, \omega^I, \theta, \theta^I)$:

$$\omega, \omega^I, \theta, \theta^I = \arg \max_{\omega, \omega^I, \theta, \theta^I} O(D; \omega, \omega^I, \theta, \theta^I), \quad (25)$$

$$O(D; \omega, \omega^I, \theta, \theta^I) := \text{LL}(D; \omega, \omega^I, \theta, \theta^I) + \alpha L_1(D; \omega) + \alpha^I L_1^I(D; \omega^I) + \beta^I \Omega(D; \omega, \omega^I, \theta, \theta^I), \quad (26)$$

$$\text{LL}(D; \omega, \omega^I, \theta, \theta^I) := \sum_{(y_k, \mathbf{x}_k) \in D} \log P(a_k | \mathbf{x}_k; \omega, \omega^I, \theta, \theta^I), \quad (27)$$

$$L_1^I(D; \omega^I) := \sum_{i \in \mathcal{A}} \sum_{(j,k) \in \mathcal{S}_i^I} |\omega_{ijk}^I|, \quad (28)$$

$$\Omega(D; \omega, \omega^I, \theta, \theta^I) := \sum_{x_i \in D} \left| \frac{1}{|\mathcal{S}_i^I|} \sum_{(j,k) \in \mathcal{S}_i^I} v_{ij}(x_{ij}; \theta_{ij}) v_{ijk}(x_{ij}, x_{ik}; \theta_{ijk}^I) \right|, \quad (29)$$

where L_1^I denotes L_1 norm for the weight ω_{ijk}^I and $\alpha^I(\leq 0)$ is the regularization parameter for the norm. $\Omega(\cdot)$ is a marginal clarity constraint representing the degree of non-orthogonality between each main effect v_{ij} and pairwise interactions v_{ijk} [29]. The constraint is necessary because v_{ij} would easily be absorbed by v_{ijk} . We optimize the problem using stochastic gradient descent methods like the Adam optimizer.

Algorithm 1 Learning MNL-GAIUNet

-
- 1: $S_i \leftarrow \{1, \dots, M\}$
 - 2: $\tilde{\omega}, \tilde{\theta} \leftarrow \arg \max_{\omega, \theta} (\text{LL}(D; \omega, \theta) + \alpha L_1(D; \omega))$
 - 3: $\tilde{S}_i \leftarrow \{i | i \in S_i, \text{Imp}(x_{ij}; \tilde{\omega}, \tilde{\theta}) \geq \text{Th}_{\text{Imp}}\}$
 - 4: $S_i^I \leftarrow \{(j, k) | j \in \tilde{S}_i, k \in \tilde{S}_i, j \neq k\}$
 - 5: $\omega^I, \theta^I = \arg \max_{\omega^I, \theta^I} (\text{LL}(D; \tilde{\omega}, \omega^I, \theta, \theta^I) + \alpha L_1(D; \omega) + \alpha^I L_1^I(D; \omega^I) + \beta^I \Omega(D; \omega, \omega^I, \theta, \theta^I))$
 - 6: $\omega, \omega^I, \theta, \theta^I = \arg \max_{\omega, \omega^I, \theta, \theta^I} (\text{LL}(D; \omega, \omega^I, \theta, \theta^I) + \alpha L_1(D; \omega) + \alpha^I L_1^I(D; \omega^I) + \beta^I \Omega(D; \omega, \omega^I, \theta, \theta^I))$
-

The importance score of the interactions is defined as follows:

$$\text{Imp}(x_{ij}, x_{ik}; \omega, \theta) := \frac{\int_{\min(x_{ij})}^{\max(x_{ij})} \int_{\min(x_{ik})}^{\max(x_{ik})} \omega_{ijk}^I v_{ijk}(x_{ij}, x_{ik}; \theta_{ijk}^I)}{(\max(x_{ij}) - \min(x_{ij}))(\max(x_{ik}) - \min(x_{ik}))}, \quad i \in \mathcal{A}, (j, k) \in S_i^I \quad (30)$$

We calculate the importance score using evenly partitioned values in the range of $\min(x_{ij})$ to $\max(x_{ij})$ and $\min(x_{ik})$ to $\max(x_{ik})$ because it would be difficult to calculate the integral directly.

Algorithm 1 shows the procedure for finding the parameters with MNL-GAIUNet. First, the parameters for the main effects are optimized based on Eq. (19) (Line 2). Then, we find the explanatory variables with greater importance score than the threshold Th_{Imp} and create the set of their variable pairs because the number of combinations of all variables is often too large for computation (Line 3-4). The assumption is premised on that the importance score of variable pairs with smaller scores would rarely be large. The parameters and weights for the pairwise interactions in MNL-GAIUNet are learned by fixing the parameters and weights of the main effect based on Eq. (25) (Line 5). Finally, we fine-tune all parameters and weights based on Eq. (25) (Line 6).

5. Experimental Setup with Trip Survey Data in Tokyo

This section introduces the experimental setup and model parameters using the trip survey data in Tokyo, Japan.

5.1. Data Summary

We evaluated our models with the trip survey data collected in Tokyo, Japan, for several months per year from 2018 through 2021. The subjects lived or worked in a waterfront district in Tokyo. The number of subjects was about 200 in 2018 and 300 in other years. The subjects recorded the travel destinations/objectives (e.g., commuting to work/school) and transport modes (e.g., train) of the trips using their smartphones. The number of trips was 12,000 in 2018, 30,000 in 2019, and 35,000 in other years. The trip destinations/objectives were *Home, Office/School, Club-Activity, Business, Meal, Leisure, Sightseeing, Pickup, Waiting*, and others. The transport modes were *Train, Walking, Subway, Bicycle, Bus, Shared-Bike, Taxi, and Others (Freight-Truck, Monorail, Motorcycle, Tram, and velotaxi)*.

We focused on the following destinations/objectives for which decision-making behavior would differ: *Office/School, Meal, Leisure, Hospital, and Sightseeing*. We also focused on the following major transport modes as alternatives: *Train, Walking, Subway, POV (Privately-Owned-Vehicle), POB (Privately-Owned-Bike), Bus, Shared-Bike, and Taxi*. We equated Train and Subway to *Train*, POB and Shared-Bike to *Bike*, and POV and Taxi to *Car*.

Table 3 shows the data overview in detail.

We present a histogram showing the ratio of trip destinations/objectives recorded and ones selected in the data in Fig. 3. The travel objective shares were almost the same in all years except for some objectives. The commuting ratio in 2018 and 2019 was more than that in 2020 and 2021, while the ratios of shopping/meal/leisure/pickup/strolling in 2018 and 2019 were less than those in 2020 and 2021. The change could have been caused by the COVID-19 pandemic. Figure 4 shows the ratio of transport modes. The mode shares were also almost the same in all years except for some modes. The ratio of public transportation, such as trains, subways, and buses, decreased after 2020 while the ratio of walking, POV, and POB increased due to the pandemic.

Figure 5 shows the number of trips recorded for each subject. The number did not change before and after the pandemic, although the number in 2018 was the lowest because of the lowest number of subjects. The number of trips was much higher for subjects below 10% than for other subjects.

Table 3
Overview of Trip Survey Data in Tokyo

Year	2018	2019	2020	2021
Subjects	people live or work at waterfront district in Tokyo			
Destination/Purpose	Home, Office/School , Shopping, Business, Meal , Leisure , Hospital , Club-Activity , Pickup, Sightseeing , Waiting, and Others			
Transport Modes	Train , Privately-Owned-Vehicles , Walking , Subway , Privately-Owned-Bike , Bus , Shared-Bike , Taxi , Freight-truck, Monorail, Motorcycle, Tram, and Velotaxi			
Period	Aug./27-Dec/31	Jul./08-2020/Mar./13	Sep./30-Dec./23	Jul./08-Nov./30
#Trips	12321	30585	35924	38490
#Trips _{selected}	3383	8266	8005	7380
#Subjects	218	316	326	325
#Subjects _{selected}	174	297	309	312

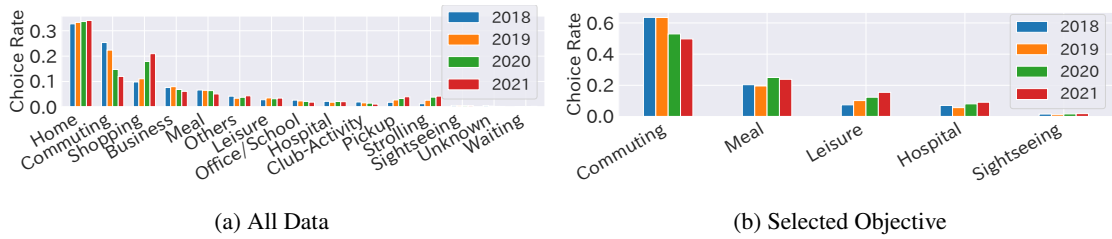


Figure 3: Histogram for travel objective in all data (a) and in the data used for the evaluation (b)

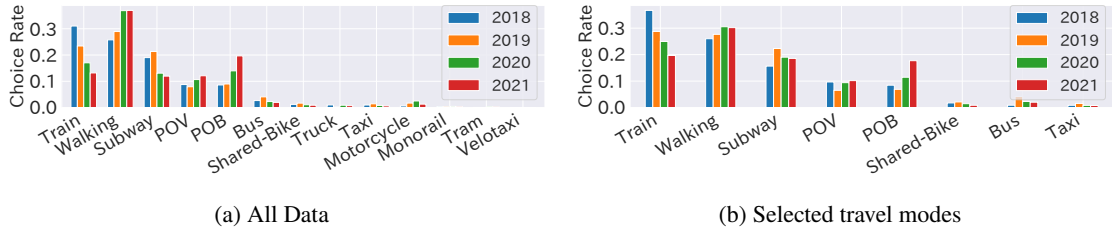


Figure 4: Histogram for travel modes

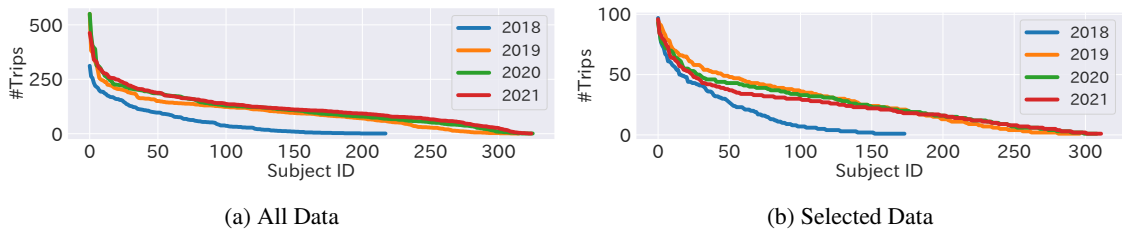


Figure 5: Total Number of Trips in all data (a) and in the recorded data for the evaluation (b)

We show the total travel time of each subject in Fig. 6. The total travel time did not change much before and after the pandemic. It can be seen that a small fraction of the subjects had a very short travel time compared to the other subjects.

5.2. Explanatory variables

In this section, we present the explanatory variables selected for the experiments. Table 4 show the list of variables recorded in the data. The travel destination/objective, time, and distance were recorded for all travel modes. The other

Discrete-Choice Model with GAIUNet

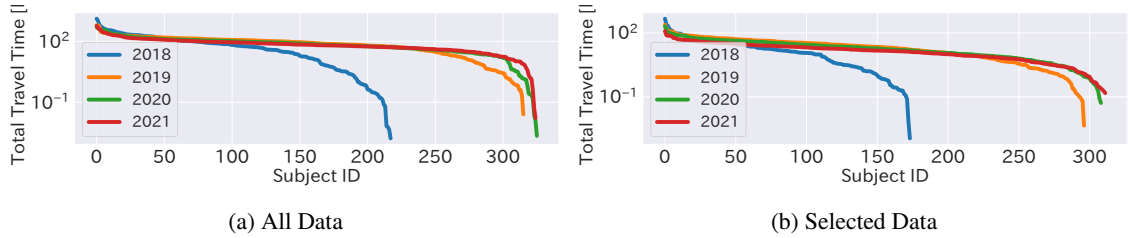


Figure 6: Total Travel Time in all data (a) and in the data recorded for the evaluation (b)

Table 4

Recorded variables and selected explanatory variables(□:recorded, ☑:selected, -:not recorded)

	Train	Bus	Car	Bike	Walking
Travel Destination/Objective	☑	☑	☑	☑	☑
Travel Time	☑	☑	☑	☑	☑
Travel Dist.	□	□	□	□	□
Cost	□	□	-	-	-
#Transits	☑	☑	-	-	-
Access Dist.	□	□	-	-	-
Access Time	☑	☑	-	-	-
Egress Dist.	□	□	-	-	-
Egress Time	☑	☑	-	-	-

variables, the cost, the number of transits, access distance, access time, egress distance, and egress time, were recorded for the train and the bus only.

We calculate the variance inflation factor (VIF), a measure that represents how much the variable can be estimated using the other variables for each explanatory variable candidate to analyze the magnitude of multicollinearity. VIF is calculated as follows:

$$\tilde{x}_i := \alpha_0^i + \sum_{j \neq i} \alpha_j^i x_j + \varepsilon^i, \forall i \in \{1, \dots, N\}, \quad (31)$$

$$R_i^2 := 1 - \frac{\sum (x_i - \tilde{x}_i)^2}{\sum (x_i - \bar{x}_i)^2}, \forall i \in \{1, \dots, N\}, \quad (32)$$

$$\text{VIF}_i := \frac{1}{1 - R_i^2}, \forall i \in \{1, \dots, N\}, \quad (33)$$

where N is the number of the explanatory variable candidates and i is its index. \tilde{x}_i is the value estimated by linear regression using the other variables $\{1, \dots, N\} \setminus i$ and \bar{x} is the mean value based on collected data \mathcal{D} . R_i^2 and VIF_i is the coefficient of determination and VIF for x_i , respectively. High VIF_i indicates that the variable set has multicollinearity because variable x_i can be accurately estimated using other variables. We selected a combination of variables so that the VIFs would be less than 10.

We selected Travel Destination/Objective, Travel Time, #Transits, Access Time, and Egress Time as the explanatory variables shown in Table 4. We confirmed that VIFs for these variables were less than 10 as shown in Table 5.

5.3. Parameters

We show the parameters for each model in Table 6. The number of layers and nodes was set to one for MNL-Linear; two layers and five nodes in each layer for the other models. We evaluated the performance with two different activation functions: hyperbolic tangent (Tanh) and LeakyReLU [16]. We set the regularization parameters, α , α^I and β^I , to 1×10^{-3} . The models with -SW represent the NN weights for the travel time that are pooled across all modes (i.e., Train, Bus, Car, Bike, and Walking). We set the batch size, and the learning rate for all models to 200 and 1×10^{-3} respectively. For MNL-GAIUNet, we use 0.1 as Th_{Imp} .

Table 5

Variance inflation factors for selected explanatory variables

	2018		2019		2020		2021	
	Train	Bus	Train	Bus	Train	Bus	Train	Bus
Travel Time	4.39	9.23	4.32	6.55	3.85	5.94	3.47	5.60
#Transits	2.78	8.81	2.57	6.43	2.27	5.28	2.02	4.84
Access Time	2.05	1.51	1.85	1.36	1.94	1.45	1.91	1.30
Egress Time	1.94	1.84	1.89	1.63	1.73	1.64	1.87	1.67

Table 6

Parameter settings in each model: MNL-Linear, MNL-Linear-SW, ASU-DNN with Tanh/LeakyReLU, MNL-GAIUNet with Tanh/LeakyReLU, and MNL-GAIUNet-SW with Tanh/LeakyReLU

	#Nodes	Activation Func.	Regularization Param.	Param. Sharing
MNL-Linear	1	-	-	-
MNL-Linear-SW	1	-	-	Travel Time[T,B,C,Bk,W] ¹
ASU-DNN(Tanh)	[5,5]	Tanh	-	-
ASU-DNN(LeakyReLU)	[5,5]	LeakyReLU	-	-
MNL-GAIUNet(Tanh)	[5,5]	Tanh	-1×10^{-3}	-
MNL-GAIUNet(LeakyReLU)	[5,5]	LeakyReLU	-1×10^{-3}	-
MNL-GAIUNet-SW(Tanh)	[5,5]	Tanh	-1×10^{-3}	Travel Time[T,B,C,Bk,W]
MNL-GAIUNet-SW(LeakyReLU)	[5,5]	LeakyReLU	-1×10^{-3}	Travel Time[T,B,C,Bk,W]
MNL-GAIUNet(Tanh)	[5,5]	Tanh	-1×10^{-3}	-
MNL-GAIUNet(LeakyReLU)	[5,5]	LeakyReLU	-1×10^{-3}	-
MNL-GAIUNet-SW(Tanh)	[5,5]	Tanh	-1×10^{-3}	Travel Time[T,B,C,Bk,W]
MNL-GAIUNet-SW(LeakyReLU)	[5,5]	LeakyReLU	-1×10^{-3}	Travel Time[T,B,C,Bk,W]

¹ T:Train, B:Bus, C:Car, Bk:Bike, W:Walking

We evaluated the performance using five fold cross-validation. In this validation method, the dataset was randomly partitioned into five equal (or nearly equal) folds. The models were trained on four folds and tested on one remaining fold. The process was performed five times, each time using a different fold. Performance was measured as the average of the log-likelihoods over the five evaluations.

6. Experimental Results

In this section, we evaluate our method in two aspects: prediction accuracy, measured by log-likelihood, and interpretability.

6.1. Prediction Accuracy

We show the log-likelihood for the models without shared network weights in Table 7. We observed that all models were learned properly because the log-likelihood of the models was much smaller than the initial log-likelihood and the difference in log-likelihood for each model between *test* and *train* was small.

We compared the performance of Tanh and LeakyReLU as activation functions in ASU-DNN, MNL-GAIUNet, and MNL-GAIUNet-SW. The result showed that Tanh was better than LeakyReLU in MNL-GAIUNet and MNL-GAIUNet-SW, while LeakyReLU was better than Tanh in ASU-DNN. This could be because the utility function approximated by ASU-DNN, which has connections between explanatory variables, was more complex than MNL-GAIUNet and MNL-GAIUNet-SW, which have no or limited connection between explanatory variables. The result was consistent with those of previous studies that ReLU family (e.g., ReLU and LeakyReLU) could achieve good performance in the approximation of complex functions (e.g., deep and large network) while classical activation functions work well in learning simple functions (e.g., shallow and small network) [5].

Table 7
Log-likelihood for the model without shared weights

	2018		2019		2020		2021	
	train	test	train	test	train	test	train	test
Initial LL	-1013	-1013	-2492	-2492	-2397	-2397	-2150	-2150
MNL-Linear	-447	-457	-1010	-1028	-1159	-1168	-1075	-1084
ASU-DNN(Tanh)	-525	-532	-1195	-1203	-1315	-1325	-1267	-1277
ASU-DNN(LeakyReLU)	-395	-413	-899	-914	-1066	-1089	-1004	-1027
MNL-GAUNet(Tanh)	-418	-427	-906	-913	-1095	-1106	-1021	-1030
MNL-GAUNet(LeakyReLU)	-442	-454	-1007	-1017	-1190	-1205	-1157	-1169
MNL-GAIUNet(Tanh)	-415	-423	-902	-909	-1094	-1104	-1020	-1031
MNL-GAIUNet(LeakyReLU)	-439	-449	-995	-990	-1175	-1178	-1156	-1168

Table 8
Log-Likelihood for the model with the shared weights

	2018		2019		2020		2021	
	train	test	train	test	train	test	train	test
Initial LL	-1013	-1013	-2492	-2492	-2397	-2397	-2150	-2150
MNL-Linear-SW	-452	-463	-1023	-1039	-1170	-1178	-1104	-1112
ASU-DNN(Tanh)	-	-	-	-	-	-	-	-
ASU-DNN(LeakyReLU)	-	-	-	-	-	-	-	-
MNL-GAUNet-SW(Tanh)	-443	-450	-978	-986	-1174	-1187	-1112	-1120
MNL-GAUNet-SW(LeakyReLU)	-435	-445	-966	-977	-1189	-1207	-1121	-1133
MNL-GAIUNet-SW(Tanh)	-441	-448	-928	-923	-1112	-1108	-1053	-1038
MNL-GAIUNet-SW(LeakyReLU)	-435	-445	-921	-915	-1178	-1200	-1109	-1115

ASU-DNN with LeakyReLU, MNL-GAUNet with Tanh, and MNL-GAIUNet with Tanh achieved better log-likelihood than MNL-Linear. The result indicated that choice policy has a nonlinear relationship with respect to the explanatory variables. MNL-GAUNet was comparable to ASU-DNN and MNL-GAIUNet. The result indicated that the interaction effect between the explanatory variables had little impact on mode choices in the experiments.

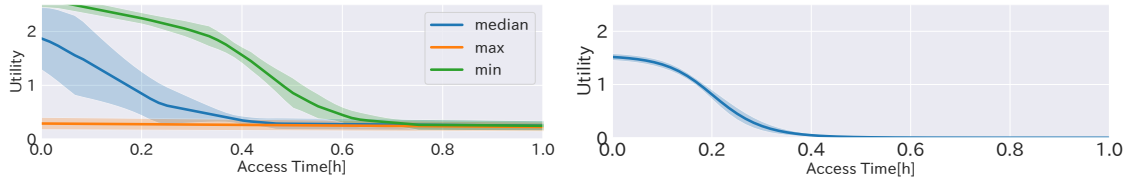
We show the log-likelihood for the model with the shared network weights of the travel time in Table 8. The results with ASU-DNN were not included because ASU-DNN cannot pool weights across alternatives owing to the neural-network architectures. We observed that all models were learned properly because the log-likelihood of the models was much smaller than the initial log-likelihood, and the difference in log-likelihood for each model between *test* and *train* was small. In the shared weights scenarios, Tanh achieved better log-likelihood than LeakyReLU as the activation function of our models in the test.

The log-likelihood for our models with shared weights was inferior to that of models with independent weights but was comparable to MNL-Linear-SW. These findings suggest that while the universal effect of travel time can be captured by linear functions, mode-specific effects may necessitate nonlinear functions.

6.2. Interpretability

We discuss the difference in interpretability between ASU-DNN and MNL-GAUNet in this subsection. When discussing the effect of the utility for an explanatory variable in ASU-DNN, we must fix the values of the other variables because the utility depends on the values of all explanatory variables. On the other hand, MNL-GAUNet can calculate the utility of each explanatory variable independently of the values of the other variables because MNL-GAUNet is modeled as a GAM. We show the utility for access time on the bus learned by these methods using the dataset in 2020 in Figure 7 as an example. The lines and the bars represent the average, and filled areas were drawn with the standard

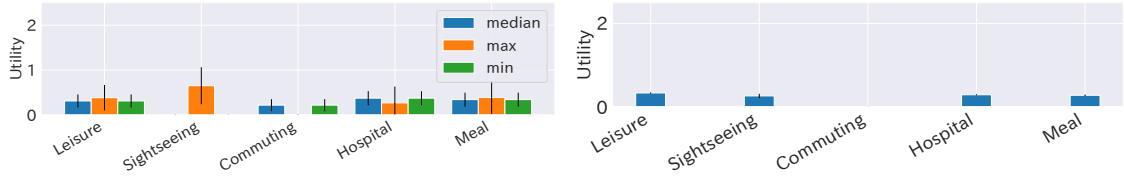
Discrete-Choice Model with GAIUNet



(a) ASU-DNN: Access Time

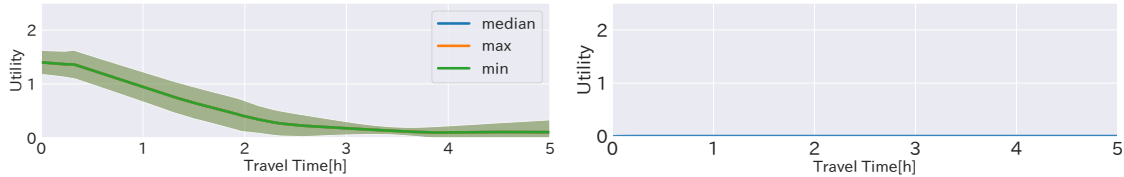
(b) MNL-GAUNet: Access Time

Figure 7: Utility for access time of buses based on ASU-DNN and MNL-GAUNet. The lines and the bars represent the average, and filled areas were drawn with the standard deviation in five folds. In Figure (a), three cases as fixed values are computed: the maximum (Orange), minimum (Green), and median values (Blue) in the dataset in ASU-DNN



(a) ASU-DNN: Objective

(b) MNL-GAUNet: Objective



(c) ASU-DNN: Travel Time

(d) MNL-GAUNet: Travel Time

Figure 8: Utility with respect to explanatory variables for Cars based on ASU-DNN and MNL-GAUNet. The lines and the bars represent the average, and filled areas were drawn with the standard deviation in five folds. In Figure (a), three cases as fixed values are computed: the maximum (Orange), minimum (Green), and median values (Blue) in ASU-DNN.

deviation in five folds. We computed three cases as fixed values: the maximum, minimum, and median values in the dataset in ASU-DNN.

Figure 7(a) shows that the utility learned by ASU-DNN varied with the fixed values while the utility learned by MNL-GAUNet was a single line in the figure 7(b). When the other variables were fixed to the minimum value, the utility was higher than the others. The nature of the dependence of utility on other values makes the analysis difficult. In contrast, the utility estimated by our method was easy to interpret because the utility is independent of the values of other explanatory variables.

We show the utilities learned by ASU-DNN and MNL-GAUNet for all explanatory variables for all transportation modes in the 2020 dataset in Figure 8 through 12. These results show that changing utilities with the values of other explanatory variables often occur in ASU-DNN: objective (Fig. 11(a)), access time (Fig. 11(e)), egress time (Fig. 11(g)), the number of transits (Fig. 11(i)) in trains, objective (Fig. 12(a)), access time (Fig. 12(e)), egress time (Fig. 12(g)) and the number of transits (Fig. 12(i)) in buses. The results show that our MNL-GAUNet can estimate the utilities with lower variance than ASU-DNN.

We can deeply understand choice behaviors using our MNL-GAUNet by capturing nonlinear effects. For example, we can observe that the decrease in utility of travel time for Car (Fig. 8(d)), Walking (Fig. 9(d)), Bike (Fig. 10(d)), and Bus (Fig. 12(d)) slows down as the distance increases¹. In the access time of trains, the difference between 0.2 and 1.0 [h] was little, while the utility in the egress time decreased linearly. The utility of the number of transfers on buses decreases faster than the number of transfers on trains (Fig.12(j), 11(j)).

¹The reason why the utility of travel time for Train increased for the time would be that many people chose trains for long-distance travel.

Discrete-Choice Model with GAIUNet

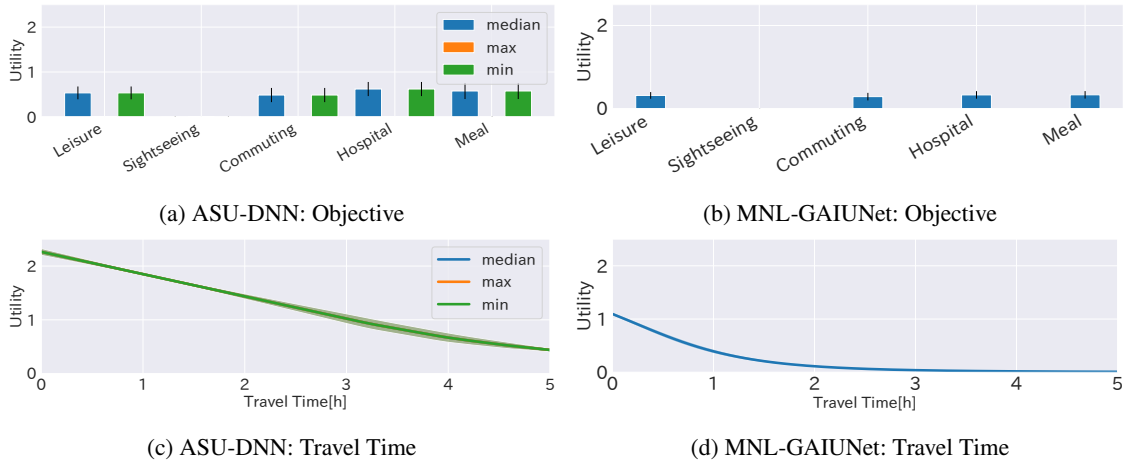


Figure 9: Utility with respect to explanatory variables for walking based on ASU-DNN and MNL-GAIUNet. The lines and the bars represent the average, and filled areas were drawn with the standard deviation in five folds. In Figure (a), three cases as fixed values are computed: the maximum (Orange), minimum (Green), and median values (Blue) in ASU-DNN.

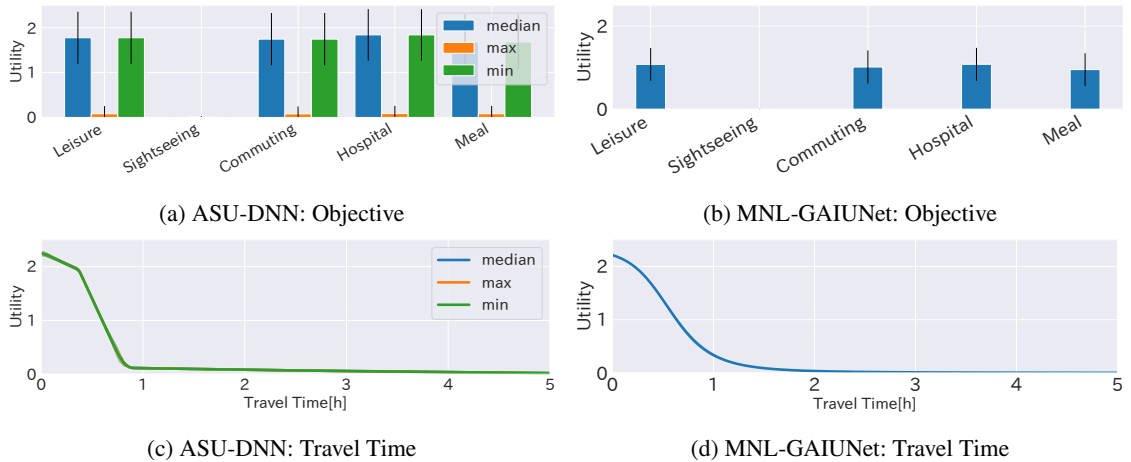


Figure 10: Utility with respect to explanatory variables for Bike based on ASU-DNN and MNL-GAIUNet. The lines and the bars represent the average, and filled areas were drawn with the standard deviation in five folds. In Figure (a), three cases as fixed values are computed: the maximum (Orange), minimum (Green), and median values (Blue) in ASU-DNN.

7. Discussion

This study developed utility functions using a novel neural-network architecture based on GAMs, GAUNet. Our approach is interpretable regarding the effect of each explanatory variable because the utility function for each variable is learned with different independent NNs. We also extended GAUNet to GAIUNet, which adds the interaction terms between two explanatory variables represented.

We evaluated MNL-GAUNet and MNL-GAIUNet with data collected in Tokyo, Japan, from 2018 to 2021. The model learned decision-making in choosing transport modes (e.g., train, bus, and car). Our models achieved prediction accuracy comparable to that of ASU-DNN, by representing utility functions using a fully connected DNN for each alternative, which improved interpretability compared to previous models.

In this study, we applied our models to transport mode choice; however, we will apply the model to more broad choice behavior modeling tasks as the next steps. In addition, our GAUNet and GAIUNet can naturally be applied to any variation of logit model families, such as (cross-)nested-logit model and latent-class model, by using our neural-network architecture as their utility functions. We will extend our model to these logit models in future work.

Discrete-Choice Model with GAIUNet

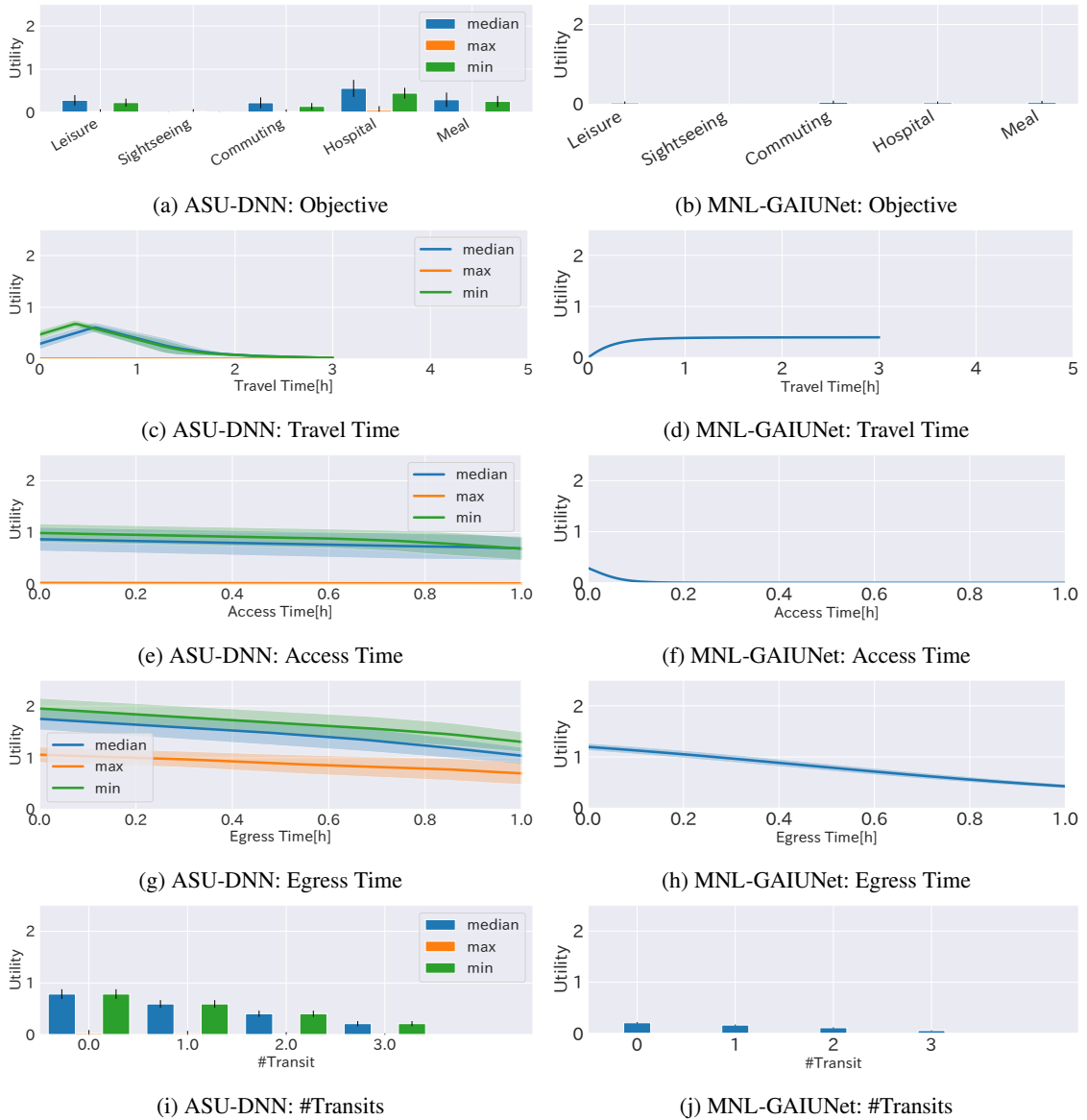


Figure 11: Utility with respect to explanatory variables for Trains based on ASU-DNN and MNL-GAIUNet. The lines and the bars represent the average, and filled areas were drawn with the standard deviation in five folds. In Figure (a), three cases as fixed values are computed: the maximum (Orange), minimum (Green), and median values (Blue) in ASU-DNN.

Acknowledgments

This work was performed as a project of Intelligent Mobility Society Design, Social Cooperation Program (Next Generation Artificial Intelligence Research Center, the University of Tokyo with Toyota Central R&D Labs., Inc.)

CRediT authorship contribution statement

Tomoki Nishi: Conceptualization of this study, Methodology, Software. **Yusuke Hara:** Conceptualization of this study, Methodology.

Discrete-Choice Model with GAIUNet

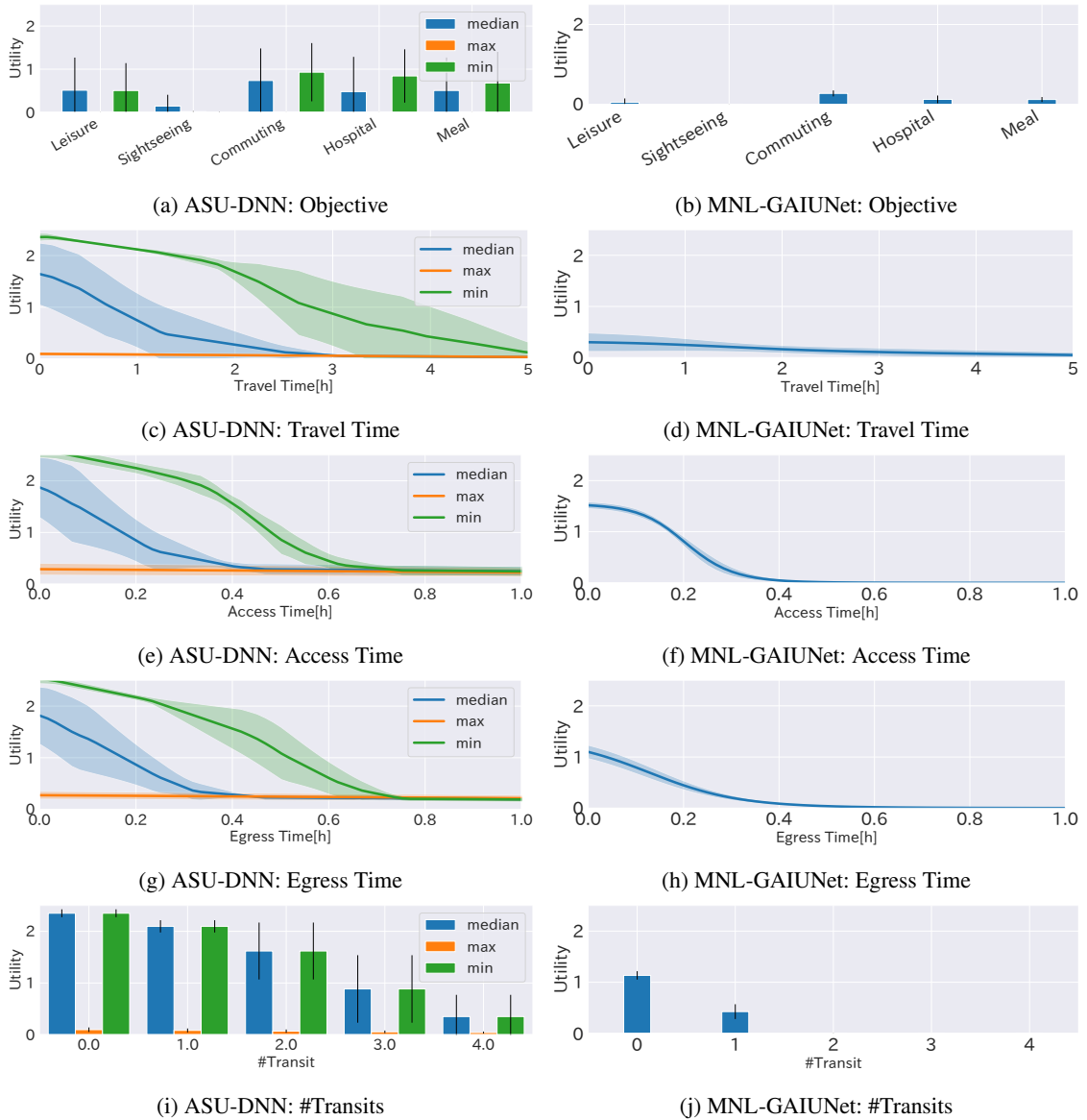


Figure 12: Utility with respect to explanatory variables for Buses based on ASU-DNN and MNL-GAIUNet. The lines and the bars represent the average, and filled areas were drawn with the standard deviation in five folds. In Figure (a), three cases as fixed values are computed: the maximum (Orange), minimum (Green), and median values (Blue) in ASU-DNN.

References

- [1] Agresti, A., 2015. Foundations of linear and generalized linear models. John Wiley & Sons.
- [2] van Cranenburgh, S., Wang, S., Vij, A., Pereira, F., Walker, J., 2022. Choice modelling in the age of machine learning-discussion paper. *Journal of Choice Modelling* 42, 100340.
- [3] Erhan, D., Bengio, Y., Courville, A., Vincent, P., 2009. Visualizing higher-layer features of a deep network. University of Montreal 1341, 1.
- [4] Fukuda, D., Yai, T., 2010. Semiparametric specification of the utility function in a travel mode choice model. *Transportation* 37, 221–238.
- [5] Glorot, X., Bordes, A., Bengio, Y., 2011. Deep sparse rectifier neural networks, in: *Proceedings of the fourteenth international conference on artificial intelligence and statistics, JMLR Workshop and Conference Proceedings*. pp. 315–323.
- [6] Greene, W.H., Hensher, D.A., 2003. A latent class model for discrete choice analysis: contrasts with mixed logit. *Transportation Research Part B: Methodological* 37, 681–698.
- [7] Gunning, D., Aha, D., 2019. Darpa’s explainable artificial intelligence (xai) program. *AI magazine* 40, 44–58.

- [8] Han, Y., Zegras, C., Pereira, F.C., Ben-Akiva, M., 2020. A neural-embedded choice model: Tastenet-mnl modeling taste heterogeneity with flexibility and interpretability. arXiv preprint arXiv:2002.00922 .
- [9] Hastie, T.J., Tibshirani, R.J., 1990. Generalized additive models. volume 43. CRC press.
- [10] Kingma, D.P., Ba, J., 2014. Adam: A method for stochastic optimization. arXiv preprint arXiv:1412.6980 .
- [11] LeCun, Y., Bengio, Y., Hinton, G., 2015. Deep learning. nature 521, 436–444.
- [12] Liu, D.C., Nocedal, J., 1989. On the limited memory bfgs method for large scale optimization. Mathematical programming 45, 503–528.
- [13] LL, T., 1927. A law of comparative judgement. Psychological Review 34, 273–286.
- [14] Lou, Y., Caruana, R., Gehrke, J., Hooker, G., 2013. Accurate intelligible models with pairwise interactions, in: Proceedings of the 19th ACM SIGKDD international conference on Knowledge discovery and data mining, pp. 623–631.
- [15] Lundberg, S.M., Lee, S.I., 2017. A unified approach to interpreting model predictions. Advances in neural information processing systems 30.
- [16] Maas, A.L., Hannun, A.Y., Ng, A.Y., et al., 2013. Rectifier nonlinearities improve neural network acoustic models, in: Proc. icml, Atlanta, GA. p. 3.
- [17] McFadden, D., Train, K., 2000. Mixed mnl models for discrete response. Journal of applied Econometrics 15, 447–470.
- [18] McFadden, D., et al., 1973. Conditional logit analysis of qualitative choice behavior .
- [19] Murphy, K.P., 2012. Machine learning: a probabilistic perspective. MIT press.
- [20] Nair, V., Hinton, G.E., 2010. Rectified linear units improve restricted boltzmann machines, in: Proceedings of the 27th international conference on machine learning (ICML-10), pp. 807–814.
- [21] Nelder, J.A., Wedderburn, R.W., 1972. Generalized linear models. Journal of the Royal Statistical Society Series A: Statistics in Society 135, 370–384.
- [22] Nori, H., Jenkins, S., Koch, P., Caruana, R., 2019. Interpretml: A unified framework for machine learning interpretability. arXiv preprint arXiv:1909.09223 .
- [23] Ribeiro, M.T., Singh, S., Guestrin, C., 2016. " why should i trust you?" explaining the predictions of any classifier, in: Proceedings of the 22nd ACM SIGKDD international conference on knowledge discovery and data mining, pp. 1135–1144.
- [24] Richard, M.D., Lippmann, R.P., 1991. Neural network classifiers estimate bayesian a posteriori probabilities. Neural computation 3, 461–483.
- [25] Sifringer, B., Lurkin, V., Alahi, A., 2020. Enhancing discrete choice models with representation learning. Transportation Research Part B: Methodological 140, 236–261.
- [26] Train, K.E., 2009. Discrete choice methods with simulation. Cambridge university press.
- [27] Vovsha, P., 1997. Application of cross-nested logit model to mode choice in tel aviv, israel, metropolitan area. Transportation Research Record 1607, 6–15.
- [28] Wang, S., Mo, B., Zhao, J., 2020. Deep neural networks for choice analysis: Architecture design with alternative-specific utility functions. Transportation Research Part C: Emerging Technologies 112, 234–251.
- [29] Yang, Z., Zhang, A., Sudjianto, A., 2021. Gami-net: An explainable neural network based on generalized additive models with structured interactions. Pattern Recognition 120, 108192.